Received September 23, 2019, accepted October 7, 2019, date of publication October 11, 2019, date of current version October 29, 2019.

Digital Object Identifier 10.1109/ACCESS.2019.2946762

A Novel Neutrosophic Subsets Definition for Dermoscopic Image Segmentation

AMIRA S. ASHOUR[1], CHUNLAI DU[2], YANHUI GUO[3], AHMED REFAAT HAWAS[1], YUPING LAI[2], AND FLORENTIN SMARANDACHE[4]

[1]Electronics and Electrical Communications Engineering Department, Tanta University, Tanta 31527, Egypt
[2]School of Information Science and Technology, North China University of Technology, Beijing 100144, China
[3]Department of Computer Science, University of Illinois at Springfield, Springfield, IL 62703, USA
[4]Mathematics Department, The University of New Mexico, Gallup, NM 87301, USA

Corresponding author: Chunlai Du (duchunlai@ncut.edu.cn)

This work was supported in part by the Natural Science Foundation of China under Grant 61702013, in part by the Joint of Beijing Natural Science Foundation and Education Commission under Grant KZ201810009011, and in part by the Science and Technology Innovation Project of North China University of Technology under Grant 19XN108.

ABSTRACT Dermoscopic images suffer from irregular and vague boundaries. New directions established the neutrosophic set (NS) approaches for clustering, and segmenting the dermoscopic images. In this work, an accurate segmentation process was developed by mapping initially the dermoscopic images to the NS domain. Thus, the neutrosophic image was defined by three subsets, namely True (T), Indeterminacy (I) and False (F). For accurate boundary detection and segmentation, different high pass (HP) filter types were used in the definition of I subset and low pass (LP) filter types in the definition of T. These filters form a new way to obtain an NS image for segmenting dermoscopy images. A comparative study was carried on the ISIC2016 skin lesion dermoscopic images dataset using different combinations of NS filter types and sizes. The results depicted the superiority of using an unsharp filter in implementing the I subset and an average filter for the T subset. 96% segmentation accuracy was reported using the proposed design compared to 92% accuracy using the default NS definition.

INDEX TERMS Neutrosophic set, dermoscopic images, unsharp filter, average filter, image segmentation.

I. INTRODUCTION

One of the most challenging tasks in healthcare is the accurate diagnosis due to the dependency on the physicians' experience along with the fuzziness in the medical images. For precise instinctive diagnosis, several medical image processing procedures, such as denoising, clustering, segmentation, and classification, have been presented based on fuzzy theory to infer the intrinsic vagueness, ambiguity, and uncertainty [1]–[3]. However, fuzzy-based approaches are sensitive to the artifacts and noise; thus, do not deliberate the pixels' spatial context [4]. To overcome this drawback, the neutrosophic concept which introduced by Smarandache as a generalization of the fuzzy set [5], [6], was applied. Generally, neutrosophic set (NS) generalizes the perception of the fuzzy-based approaches including the fuzzy set, and intuitionistic fuzzy set [7].

The associate editor coordinating the review of this manuscript and approving it for publication was Md. Asikuzzaman.

By integrating medical image analysis with the NS, several computer-aided diagnosis (CAD) systems have been developed in the clinical care. Accordingly, researchers developed different NS-based medical image segmentation methods for lesions and abnormalities detection in CAD systems [8]–[12]. Cheng and Guo [13] applied a thresholding based segmentation method after transforming the image in the NS domain. The three NS subsets, namely True (T), Indeterminacy (I), and False (F) were generated. Then, the entropy in NS was calculated to estimate the indetermination. In addition, to reduce the set's indetermination, an λ-mean operation was employed. Sert and Alkan [14] designed NS-based Chan–Vese segmentation approach for edge detection. Zhang *et al.* [15] applied the neutrosophy theory for image segmentation by mapping the image in the NS domain and employed a watershed approach to segment the image.

Furthermore, several studies were conducted on the clustering-based segmentation algorithm using NS. Shan *et al.* [16] proposed NS-based clustering procedure,

called neutrosophic L-means (NLM) for segmentation. In NS domain, Guo and Cheng [9] introduced fuzzy c-means clustering, where the entropy was used to calculate the indeterminacy of the image. An α-mean operator was proposed for diminishing the indeterminacy to guarantee homogenous image. Subsequently, the membership value in the fuzzy c-means clustering was updated in consistent with the indeterminacy value to obtain the segmented image. Moreover, Guo and Sengur [17] redefined a clustering convergence criterion by integrating NS with an improved fuzzy c-means (IFCM). Further, the same authors introduced the fuzzy c-means clustering with NS context [18]. This procedure was named neutrosophic c-means (NCM), where the clustering procedure was considered a constrained minimization problem of a pre-defined objective function. Another clustering-based segmentation, namely K-means was integrated with the NS by Mohan *et al*. [19], where a non-local neutrosophic wiener filter was designed to enhance the image quality. Recently, Ashour *et al*. [20] proposed a neutrosophic clustering with histogram estimation for dermoscopic image segmentation. Histogram-based cluster estimation was implemented firstly to determine the initial number of clusters in the image, and then the NCM algorithm was applied for segmentation.

In the previous NS-based studies, median filter and Sobel filter were used in the NS to implement the truth subset, and indeterminacy subset, respectively. For accurate boundary detection and segmentation, the present work designed a novel implementation of the T and I neutrosophic subsets to guarantee the superior segmentation performance for dermoscopic image. Subsequently, a comparative study was conducted on the size and type of the proposed NS filters that compute the T and I neutrosophic subsets in the NS. Different high-pass (HP) filters were employed to compute the I subset, namely Prewitt, Sobel, kernel, double kernel, and unsharp with different filter sizes. Moreover, different low-pass (LP) filters were tested to obtain the T subset, namely median, average, and order rank filters (minimum, maximum). The k-means clustering process was utilized for segmentation based on the values in T and I. The proposed new NS subsets were evaluated to segment the dermoscopic images' lesions in the International Skin Imaging Collaboration (ISIC) 2016 Challenge dataset [21].

The structure of the rest sections is as follows. Section II presents a new methodology for defining the neutrosophic subsets. Section III contains the detailed results, comparative studies and discussion. The conclusion of the present work is denoted in section IV.

II. METHODOLOGY

The dermoscopic images have inconsistent structures and suffer from asymmetrical and ambiguous boundaries along with the existence of artifacts, noise, hair and air bubbles. For precise analysis of skin lesions, several researchers transformed the dermoscopic images into the NS domain to solve the uncertainty and indeterminacy during the segmentation process and to detect the boundaries of the lesion correctly [24], [25]. In this work, the k-means clustering is employed for segmenting the skin lesions' orbicular shape and groups the pixels of the image into different clusters. However, to increase the performance of the k-means, a new definition of the NS filters is introduced to guarantee the accurate boundary detection.

Usually, the HP filters are used for image enhancement, while the LP filters are used for smoothing and noise suppression. Accordingly, the traditional definitions of the NS subsets employed Sobel filter for computing the I subset, and a median filter for representing the T subset [10], [17]–[20]. Typically, the unsharp filter has better performance to enhance and sharpen the high frequency components in the images compared to other HP filters, such as Prewitt, Sobel, and kernel operators [22]. Moreover, the average (which is linear filter) filter has good performance and high speed compared to the median (which is a non-linear filter) in image processing and analysis [23]. Subsequently, in the present work, a new combination of the filters was proposed, where unsharp filter and average filter were used to define the I and T subsets, respectively. Likewise, the window size of each filter was determined along with a comparative study with other filter types. To evaluate the novel definition in the NS subsets for the segmentation process, the ISIC 2016 dataset was employed in this work.

A. NEUTROSOPHIC IMAGE

NS describes the indeterminacy and uncertainty in any environment. In the NS, three neutrosophic subsets, i.e. T, I, and F are defined for any event to represent the degrees of truth, indeterminacy, and falsity, respectively. These subsets are used to transform an image into the NS space creating a neutrosophic image, which is represented as $< T, I, F >$.

Typically, the default NS was defined using Sobel filter and median filter. The proposed work designed a new NS definition on the dermoscopic images, where T represents the skin lesion region, while I represents the lesion boundary information, and F represents the background. Using the minimum and maximum intensities $V_{\min}$ and $V_{\max}$, the T and F neutrosophic subsets are represented as follows [20], [25]:

$$T(l,m) = \frac{V(l,m) - V_{\min}}{V_{\min_{\max}}} \tag{1}$$

$$F(l,m) = 1 - T(l,m) \tag{2}$$

where for each pixel $V(l,m)$ in an image V, the three subsets are given by $\{T(l,m), I(l,m), F(l,m)\}$ in the neutrosophic image. Furthermore, using the local average intensity $\varepsilon(l,m)$, the I neutrosophic subset is given by:

$$I(l,m) = \frac{\varepsilon(l,m) - \varepsilon_{\min}}{\varepsilon_{\min_{\max}}} \tag{3}$$

where ε_{min} and ε_{max} are the minimum and maximum absolute difference values, respectively, of the local mean-value, and $\varepsilon_{\min_{\max}}$ represents the difference between them. A HP filter

$H(a, b)$ is applied to calculate the indeterminacy of the NS image.

In NS, the entropy specifies the pixels distribution in the neutrosophic image. The entropy of I is measured using the following expression:

$$Ent_I = -\sum_{i=min\{I\}}^{max\{I\}} pr_I\,(i) ln(pr_I\,(i)) \tag{4}$$

where $pr_I\,(i)$ is probability of the pixel in the I subset. Consequently, the entropy of I is used to associate T and F with I.

B. PROPOSED NEUTROSOPHIC SET DEFINITION AND SEGMENTATION APPROACH

1) UNSHARP FILTER FOR I SUBSET DEFINITION

For precise mapping of the dermoscopic images into NS domain, it is indispensable to select the type and size of the HP filter for calculating the indeterminacy of the neutrosophic image. Unlike the Sobel filter which used in the previous studies of NS [20], [25], the unsharp filter is an accurate sharpening operator that augments the high-frequency components and boundary information [26]. Hence, in the proposed work, an unsharp operator $H_{Unsharp}$ is used to represent the $H(a, b)$ during the calculations of the I subset in equations 3 and 4. Furthermore, a comparative study using different HP filters is conducted to determine the best filter design for calculating the I subset.

By applying the unsharp filter on an image $O(x, y)$, the formed gradient image $P(x, y)$ is stated as:

$$P(x, y) = O(x, y) - O_{lowpass}(x, y) \tag{5}$$

where $O_{lowpass}(x, y)$ is the processed $O(x, y)$ image using the LP filter. For refining, the high frequency component is added back to the original image as follows:

$$O_{Unsharp}(x, y) = O(x, y) + c * P(x, y) \tag{6}$$

where c is a scaling constant. The unsharp filter $H_{Unsharp}$ with size 3×3 can be represented as:

-1/16	-2/16	-1/16
-2/16	12/16	-2/16
-1/16	-2/16	-1/16

In addition, the $H_{Unsharp}$ of size 5×5 is represented as:

-1/32	0	-2/32	0	-1/32
0	-1/32	-2/32	-1/32	0
-2/32	-2/32	24/32	-2/32	-2/32
0	-1/32	-2/32	-1/32	0
-1/32	0	-2/32	0	-1/32

Therefore, the I subset is defined for each pixel in the NS domain using the proposed $H_{Unsharp}$.

2) AVERAGE FILTER FOR T SUBSET DEFINITION

The subset I is used to find the pixels that will be considered while modifying the subset T in the next version NS finding. Typically, the average filter is a linear spatial filter which computes the pixels' average in the mask neighborhood. This averaging process reduces the sharp transition in the image's intensities. Accordingly, the local mean $T(l, m)$ can be expressed using this average filter as follows:

$$T_{local\_average}(l, m) = \frac{1}{s \times s} \sum_{a=m-s/2}^{m+s/2} \sum_{b=l-s/2}^{l+s/2} V(a, b) \tag{7}$$

where $V(a, b)$ is the local image that filtered by $H(a, b)$, and s is the filter size. In the α-mean operation, a LP (average filter) is employed to calculate the true subset of the neutrosophic image, and then T is modified according to the values of I. To use α-mean operation iteratively for updating T, the I is used to determine the pixels that will be taken α-mean operation. This α-mean operation used a threshold value α to identify the pixels for updating the used pixels' intensity in T as follows:

$$T_{updated}(l, m) = \begin{cases} T_{local\_average}(l, m), & I(l, m) > \alpha \\ T(l, m), & I(l, m) \leq \alpha \end{cases} \tag{8}$$

Then, $T_{updated}(l, m)$ is used to produce the new updated NS image using the following formula:

$$V_{modified}(l, m) = Vupdatedminmax_{min} \tag{9}$$

Finally, the entropy of I is used as a terminating criterion of the iterative process using a threshold δ, which is given by:

$$\frac{Ent_I(i) - Ent_I(i+1)}{Ent_I(i)} < \delta \tag{10}$$

From the preceding methodology, the new definition of the NS subset is proposed. For the dermoscopic images segmentation, I subset used an unsharp (HP) filter for boundary detection of the skin lesion. Then, based on the α_{mean}, which are used in the updating of the final version of the T image in the NS. In the present work, for skin lesion segmentation, a dermoscopic image enhancement using hair removal was conducted. Then, the red channel of the RGB image, which contains all information about lesion, was transformed to the NS domain using the new NS definition. The generated components of the neutrosophic image are used to cluster the pixels of the dermoscopic images. A threshold value is used to update the T subset to obtain the modified version based on the computed I subset. Then, the k-means clustering process was applied for segmentation based on the values in T and I.

III. EXPERIMENTAL RESULTS AND DISCUSSION

In this section, different filters were used to implement I and T subsets to compare the proposed new NS filters with combinations of different filters for evaluating the performance of the proposed NS filters design (definition). Thus, for this comparative study, Prewitt, Sobel, kernel, double kernel and unsharp filters with different sizes were used in the design of the HP filters of the I subset. Additionally, another different LP filters' design for the T subset were used, namely median, average, and order filter (minimum, and maximum). Figure 1 illustrated the initial steps before using the NS filter on images.

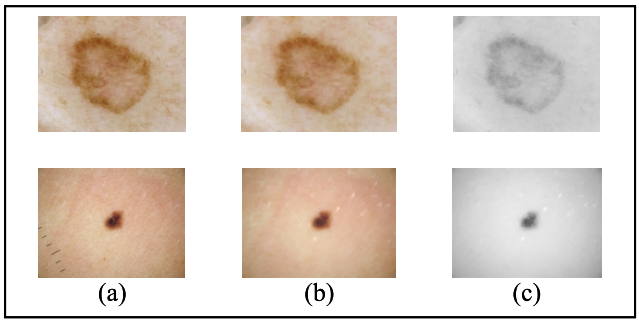

FIGURE 1. Initial pre-processing steps: (a) original images number ISIC_0000153 and ISIC_0011082 at the upper row and the lower row, respectively, (b) after hair removal filter, and (c) red channel of the filtered image.

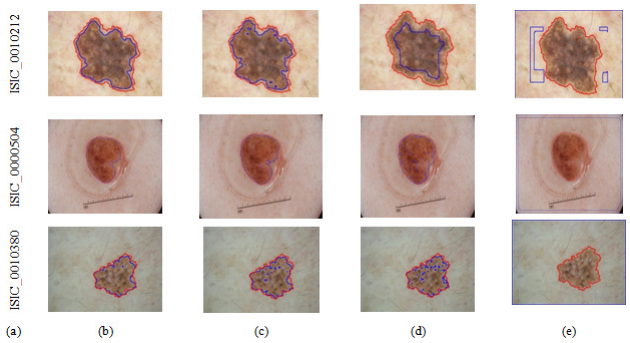

FIGURE 2. Comparative study of the different combinations for designing the NS filter for the images with numbers in (a), where (b) proposed unsharp of size 5 × 5 with average filter of size 3 × 3, (c) kernel of 9 × 9 with median filter of 3 × 3, (d) double kernel of 9 × 9 with maximum order filter of size 3 × 3, and (e) unsharp of size 5 × 5 with minimum order filter of size 3 × 3.

Different combinations of filters are used, and results are compared visually in Figure 2, which displayed the final segmented skin lesion images. These combinations are unsharp filter of size 5 × 5 with average filter of size 3 × 3, kernel filter of 9 × 9 with median filter of 3 × 3, double kernel filter of size 9 × 9 with maximum order filter of size 3 × 3, and unsharp filter of size 5 × 5 with minimum order filter of size 3 × 3.

Figure 2 established that the best combinations consist of using unsharp filter of size 5 × 5 with average filter of size 3 × 3, or Laplacian kernel of 9 × 9 with median filter of 3 × 3. However, using the unsharp of size 5 × 5 with average filter of size 3 × 3 provided more smooth borders compared to using the kernel of 9 × 9 with median filter of 3 × 3. Accordingly, Figures 3 demonstrated a comparison between the unsharp of size 5 × 5 with average filter of size 3 × 3 commination, and the kernel of 9 × 9 with median filter of 3 × 3 combinations in terms of the NS steps for an example using the image ISIC_0000153, respectively.

To evaluate the performance of the new NS filters design, 90 dermoscopy images from the ISIC2016 skin lesion dermoscopic images were used. The segmentation performance was evaluated by measuring several metrics, including the Dice coefficient (Dice), JAC, accuracy, specificity,

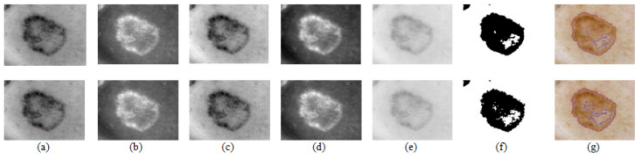

FIGURE 3. Comparative study in terms of the steps of the NS to obtain the segmented image using the proposed unsharp of size 5 × 5 with average filter of size 3 × 3 combination at the first row, and the Kernel of 9 × 9 with median filter of 3 × 3 at the second row of the figure for image number ISIC_0000153, where (a) initial T image, (b) initial F image, (c) last T version after the NS iterations, (d) Last F version after the last NS iterations, (e) final NS output, (f) k-means output, and (g) the final segmented image.

TABLE 1. Segmentation results comparison of different combinations.

NS filters combination	JAC	Dice	Sensitivity	Specificity	Accuracy
Double Kernel 9x9 with Maximum order filter 3x3	0.69	0.79	0.71	0.97	0.92
Unsharp 5x5 with Minimum order filter 3x3	0.70	0.79	0.82	0.87	0.87
Kernel 9x9 with Median 3x3	0.82	0.89	0.82	0.99	0.95
Unsharp 5x5 with Average 3x3 [Proposed]	0.83	0.91	0.83	0.99	0.96

and sensitivity [20]. The Dice measures the association between S_1 and S_2 is given by:

$$Dice = \frac{2|S_1 \cap S_2|}{|S_1| + |S_2|} \tag{11}$$

where $\cup$ and $\cap$ are the union and intersection operations, respectively. Additionally, the JAC for J_1 and J_2 is defined by:

$$JAC(J_1, J_2) = \frac{J_1 \cap J_2}{J_1 \cup J_2} \tag{12}$$

where J_1 and J_2 are the segmented and ground-truth images, respectively. The other metrics include accuracy which measures the ratio between the negative and positive results; specificity which measures how the segmentation method predicts the other regions in the image; and sensitivity which measures the detection capability of the segmentation method for detecting the lesion regions. Table 1 and Figure 4 reported the average evaluation metrics over the used dataset images using different combinations, where the ISIC2016 dataset includes different sizes of skin lesion dermoscopic images.

The results in Table 1 established the superiority of the used new NS filters definition even the used images have different images' sizes.

Table 1 and Figure 4 established the superiority of the proposed unsharp 5×5 with average 3×3 combination for the NS filter design compared to the other combinations in terms of the measured evaluation metrics. In addition, the computational time of the NS with the different combinations are reported in Figure 5.

However, the average computational time of the NS using the different combinations stated that the unsharp 5 × 5

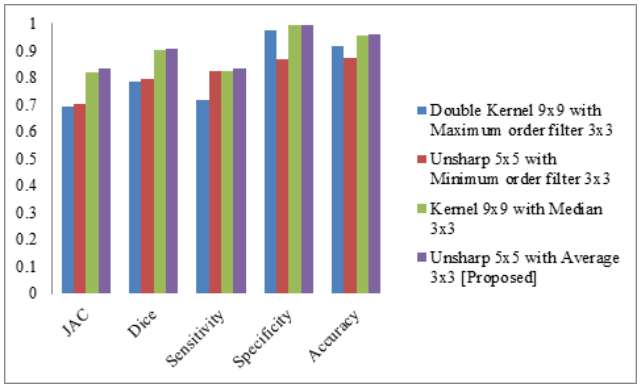

FIGURE 4. Comparison in terms of the average evaluation metrics over 90 images using different combinations followed by k-means.

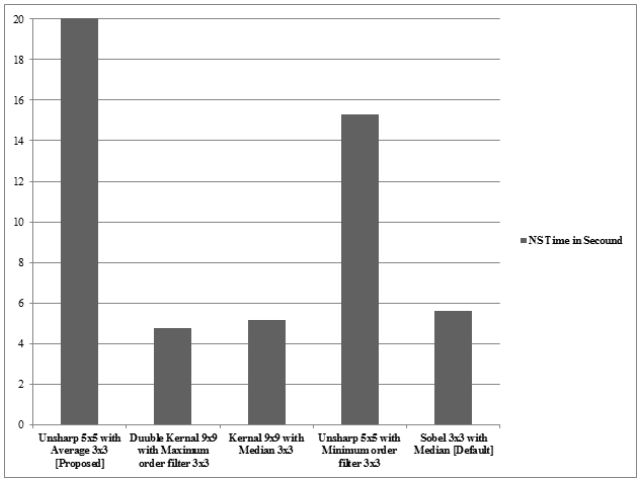

FIGURE 5. Comparison in terms of the average computational time in seconds over 90 images using different combinations followed by k-means and using in the traditional k-means and GC methods.

with average 3×3 took the maximum computational time of 22.07 seconds, while the kernel 9×9 with median 3×3 took less computational time of 5.17 seconds during the NS process. The double kernel 9×9 with maximum order filter 3×3 followed by k-means requires the least time during the NS process of 4.78 seconds in comparison to using the other NS combinations. Another comparison in terms of the different evaluation metrics using the traditional graph-cut, k-means and the NS default filters (Sobel 3×3 with median 3×3) followed by k-means in comparison with the proposed combinations of the NS filters followed by the k-means is described in Table 2.

Table 2 illustrated the superiority of the proposed NS definition for skin lesion segmentation. Accordingly, it is recommended in the future work to integrate the proposed NS definition with other segmentation methods. Moreover, the proposed definition can be tested with different medical images from different modalities, including microscopic images, ultrasound images, and magnetic resonance images to find the utmost appropriate NS definitions.

TABLE 2. Comparison between the traditional segmentation methods with the proposed NS filters in terms of the average evaluation metrics.

Segmentation method	JAC	Dice	Sensitivity	Specificity	Accuracy
Graph-cut (GC)	0.62	0.72	0.70	0.91	0.89
K-means	0.75	0.79	0.79	0.94	0.91
Default NS using Sobel 3x3 Median followed by K-means	0.79	0.80	0.79	0.95	0.92
Proposed NS using unsharp 5x5 with average 3x3 followed by K-means	0.83	0.91	0.83	0.99	0.96

IV. CONCLUSION

Edge detection and segmentation are significant steps for accurate recognition of skin lesion diseases in automated diagnostic systems. Due to the fuzziness, irregular shape, and intra-class inconsistency of the lesion boundaries, recently NS is employed efficiently in skin lesion segmentation. Since the NS depends mainly on its three subsets, namely T, I, and F, using different definitions of the NS filters have a great impact on the performance of the NS in image processing.

This work introduced new definitions of the NS subset and improved the overall performance of skin lesion segmentation in dermoscopic images. An experiment was taken on the proposed definition with different filters' combinations including the default filter of using Sobel with median filter. In addition, other combinations and segmentation methods, such as GC and k-means were examined. Furthermore, several evaluation metrics were measured on the images from the public ISIC2016 dataset.

The results established the superiority of the proposed combination using unsharp 5×5 with average 3×3 which achieved the best measured metric values of 96% accuracy, 99% specificity, and 83% sensitivity as well as 0.91 Dice and 0.83 JAC. However, the proposed design took the longest computational time of 22.07 seconds compared to the other combinations.

In future, a new dermoscopic image segmentation approach based on the proposed NS definition can be improved with other segmentation methods. Moreover, the same proposed segmentation algorithm can be used for segmenting in different medical applications including advanced diseases' images and identify the diseases as well as this new NS filters representation can be generalized with natural images dataset of different sizes.

REFERENCES

[1] H. Bustince, E. Barrenechea, M. Pagola, J. Fernandez, Z. Xu, B. Bedregal, J. Montero, H. Hagras, F. Herrera, and B. B. De, "A historical account of types of fuzzy sets and their relationships," *IEEE Trans. Fuzzy Syst.*, vol. 24, no. 1, pp. 179–194, Feb. 2016.

[2] H. Wang, Z. Xu, and W. Pedrycz, "An overview on the roles of fuzzy set techniques in big data processing: Trends, challenges and opportunities," *Knowl.-Based Syst.*, vol. 118, pp. 15–30, Feb. 2017.

[3] M. A. Sodenkamp, M. Tavana, and D. Di Caprio, "An aggregation method for solving group multi-criteria decision-making problems with single-valued neutrosophic sets," *Appl. Soft Comput.*, vol. 71, pp. 715–727, Oct. 2018.
[4] G. Liu, Y. Zhang, and A. Wang, "Incorporating adaptive local information into fuzzy clustering for image segmentation," *IEEE Trans. Image Process.*, vol. 24, no. 11, pp. 3990–4000, Nov. 2015.
[5] F. Smarandache, *A Unifying Field in Logics: Neutrosophic Logic. Neutrosophy, Neutrosophic Set, Neutrosophic Probability*. Coimbatore, India: Infinite Study; 2005.
[6] F. Smarandache, "Neutrosophic set—A generalization of the intuitionistic fuzzy set," *J. Defense Resour. Manage.*, vol. 1, no. 1, pp. 107–116, 2010.
[7] S. Broumi and F. Smarandache, "Correlation coefficient of interval neutrosophic set," *Appl. Mech. Mater.*, vol. 436, pp. 511–517, Oct. 2013.
[8] H. D. Cheng, Y. Guo, and Y. Zhang, "A novel image segmentation approach based on neutrosophic set and improved fuzzy C-means algorithm," *New Math. Natural Comput.*, vol. 7, no. 1, pp. 155–171, Mar. 2011.
[9] Y. Guo and H. D. Cheng, "New neutrosophic approach to image segmentation," *Pattern Recognit.*, vol. 42, no. 5, pp. 587–595, May 2009.
[10] Y. Guo, A. Şengür, and J. W. Tian, "A novel breast ultrasound image segmentation algorithm based on neutrosophic similarity score and level set," *Comput. Methods Programs Biomed.*, vol. 123, pp. 43–53, Jan. 2016.
[11] H. D. Cheng, J. Shan, W. Ju, Y. Guo, and L. Zhang, "Automated breast cancer detection and classification using ultrasound images: A survey," *Pattern Recognit.*, vol. 43, no. 1, pp. 299–317, Jan. 2010.
[12] M. Ali, L. H. Son, M. Khan, and N. T. Tung, "Segmentation of dental X-ray images in medical imaging using neutrosophic orthogonal matrices," *Expert Syst. Appl.*, vol. 91, pp. 434–441, Jan. 2018.
[13] H. D. Cheng and Y. Guo, "A new neutrosophic approach to image thresholding," *New Math. Natural Comput.*, vol. 4, no. 3, pp. 291–308, Nov. 2008.
[14] E. Sert and A. Alkan, "Image edge detection based on neutrosophic set approach combined with Chan-Vese algorithm," *Int. J. Pattern Recognit. Artif. Intell.*, vol. 33, no. 3, Mar. 2019, Art. no. 1954008.
[15] M. Zhang, L. Zhang, and H. D. Cheng, "A neutrosophic approach to image segmentation based on watershed method," *Signal Process.*, vol. 90, no. 5, pp. 1510–1517, 2010.
[16] J. Shan, H. D. Cheng, and Y. Wang, "A novel segmentation method for breast ultrasound images based on neutrosophic l-means clustering," *Med. Phys.*, vol. 39, no. 9, pp. 5669–5682, 2012.
[17] Y. Guo and A. Sengur, "A novel color image segmentation approach based on neutrosophic set and modified fuzzy C-means," *Circuits, Syst., Signal Process.*, vol. 32, no. 4, pp. 1699–1723, Aug. 2013.
[18] Y. Guo and A. Sengur, "NCM: Neutrosophic C-means clustering algorithm," *Pattern Recognit.*, vol. 48, no. 8, pp. 2710–2724, Aug. 2015.
[19] J. Mohan, V. Krishnaveni, and Y. Huo, "Automated brain tumor segmentation on MR images based on neutrosophic set approach," in *Proc. 2nd Int. Conf. Electron. Commun. Syst. (ICECS)*, Feb. 2015, pp. 1078–1083.
[20] A. S. Ashour, Y. Guo, E. Kucukkulahli, P. Erdogmus, and K. Polat, "A hybrid dermoscopy images segmentation approach based on neutrosophic clustering and histogram estimation," *Appl. Soft Comput.*, vol. 69, pp. 426–434, Aug. 2018.
[21] *International Skin Imaging Collaboration*. Accessed: Aug. 14, 2019. [Online]. Available: http://www.isdis.net/index.php/isic
[22] W. F. Schreiber, "Image processing for quality improvement," *Proc. IEEE*, vol. 66, no. 12, pp. 1640–1651, Dec. 1978.
[23] A. Cichocki and S. I. Amari *Adaptive Blind Signal and Image Processing: Learning Algorithms and Applications*. Hoboken, NJ, USA: Wiley, 2002.
[24] T. Matsumoto and A. Taguchi, "Removal of impulse noise from highly corrupted images by using noise position information and directional information of image," *Proc. SPIE*, vol. 4304, pp. 188–196, May 2001.
[25] A. S. Ashour, A. R. Hawas, Y. Guo, and M. A. Wahba, "A novel optimized neutrosophic *k*-means using genetic algorithm for skin lesion detection in dermoscopy images," *Signal, Image Video Process.*, vol. 12, no. 7, pp. 1311–1318, Oct. 2018.
[26] Y. Guo, A. Ashour, and F. Smarandache, "A novel skin lesion detection approach using neutrosophic clustering and adaptive region growing in dermoscopy images," *Symmetry*, vol. 10, no. 4, p. 119, Apr. 2018.
[27] C. Solomon and T. Breckon, *Fundamentals of Digital Image Processing: A practical approach with examples in Matlab*. Hoboken, NJ, USA: Wiley, 2011.

AMIRA S. ASHOUR received the B.S. degree in electrical engineering [electronics and electrical communications engineering (EEC)] from the Faculty of Engineering, Tanta University, Egypt, in 1997, the M.Sc. degree in image processing for nondestructive evaluation performance from the EEC Department, Faculty of Engineering, Egypt, in 2000, and the Ph.D. degree in smart antenna (direction of arrival estimation using local polynomial approximation) from the Faculty of Engineering, Tanta University, in 2005. She was the Vice-Chair of the Computer Engineering Department, Computers and Information Technology College (CIT), Taif University, KSA, from 2015 to 2016, where she was also the Vice-Chair of the Computer Science Department, until 2015. She has been an Assistant Professor and the Head of the EEC Department, Faculty of Engineering, Tanta University, since 2016, where she is currently a member of the Research and Development Unit. She has 20 edited books and four authored books along with about 170 outstanding published articles in repute journals and conferences. Her research interests include image processing and analysis, medical imaging, computer-aided diagnosis, signal/image/video processing, machine learning, smart antenna, direction of arrival estimation, targets tracking, inverse problems, optimization, and neutrosophic theory. She is the Editor-in-Chief for the *International Journal of Synthetic Emotions* (IJSE), IGI Global, USA. She is also an Associate Editor in several international journals. She is also Series Co-Editor of *Advances in Ubiquitous Sensing Applications for Healthcare series*, (Elsevier).

CHUNLAI DU received the Ph.D. degree in computer architecture from the Harbin Institute of Technology, China, in 2009. He is currently an Associate Professor with the North China University of Technology, China. His research interests include network security, machine learning, and data mining.

YANHUI GUO received the B.S. degree in automatic control from Zhengzhou University, China, in 1999, the M.S. degree in pattern recognition and intelligence system from the Harbin Institute of Technology, China, in 2002, and the Ph.D. degree from the Department of Computer Science, Utah State University, USA, in 2010. He was a Research Follow with the Department of Radiology, The University of Michigan, and an Assistant Professor with St. Thomas University. He is currently an Assistant Professor with the Department of Computer Science, University of Illinois at Springfield. He has published more than 90 journal articles, 30 top conference papers, and completed more than ten grant funded research projects. His research interests include computer vision, machine learning, big data analytics, computer-aided detection/diagnosis, and computer assist surgery. He was an Associate Editor of different international journals and a Reviewer for top journals and conferences.

AHMED REFAAT HAWAS received the B.Sc. degree in electrical engineering from the Faculty of Engineering, Tanta University, Egypt, in 2010, and the M.Sc. degree in electronics and electrical communications engineering (computer vision) from the Faculty of Engineering, Tanta University, in 2017. He joined the nine-month Diploma degree in software engineering (UNIX) at the Information Technology Institute (ITI), in 2011. He has appointed as a Demonstrator in electronics and electrical communications engineering at Tanta University, in 2010, where he is currently an Assistant Lecturer. He has several published academic articles in repute journals. His research interests include video/image processing, medical imaging, deep learning, pattern recognition, image analysis, computer vision, and optimization.

YUPING LAI received the Ph.D. degree in information security from the Beijing University of Posts and Telecommunications, Beijing, China, in 2014. He has been an Associate Professor with the North China University of Technology, China, since 2014. His research interests include information security, computer vision, pattern recognition, machine learning, and data mining.

FLORENTIN SMARANDACHE received the M.Sc. degree in mathematics and computer science from the University of Craiova, Romania, and the Ph.D. degree in mathematics from the State University of Kishinev, and the Ph.D. degree in applied mathematics from the Okayama University of Sciences, Japan. He has been the Founder of neutrosophy (generalization of dialectics), neutrosophic set, logic, probability, and statistics, since 1995. He is currently a Professor of mathematics with the University of New Mexico, USA. He has published hundreds of articles on neutrosophic physics, superluminal and instantaneous physics, unmatter, absolute theory of relativity, redshift and blueshift due to the medium gradient and refraction index besides the Doppler effect, paradoxism, outerart, neutrosophy as a new branch of philosophy, law of included multiple-middle, multispace and multistructure, degree of dependence and independence between neutrosophic components, refined neutrosophic set, neutrosophic over-under-off-set, plithogenic set, neutrosophic triplet and duplet structures, quadruple neutrosophic structures, DSmT, and so on to many peer-reviewed international journals and many books and he presented articles and plenary lectures to many international conferences around the world.